Improved Figure of Merit of (Ba,Sr)TiO$_3$-Based Ceramics by Sn Substitution

Jong-Yoon Ha, Liwei Lin, Dae-Yong Jeong[1], Seok-Jin Yoon[2], and Ji-Won Choi[2]*

Mechanical Department, University of California at Berkeley, Berkeley, CA 94720, U.S.A.
[1]*Department of Materials Science and Engineering, Myongji University, Yongin, Gyeonggi-do 449-728, Korea*
[2]*Thin Film Materials Research Center, KIST, Seoul 130-650, Korea*

The dielectric properties of (Ba$_{0.6}$Sr$_{0.4}$)(Ti$_{1-x}$Sn$_x$)O$_3$ (0 ≤ x ≤ 0.3) ceramics were investigated. Single-phase specimens having a cubic perovskite structure could be obtained. As Sn concentration increased, dielectric loss decreased untill a composition of $x = 0.15$ and slightly increased as Sn concentration increased further. The diffused phase transition appeared owing to substitution of Sn ions. When Sn was substituted at 0.1 mol in (Ba$_{0.6}$Sr$_{0.4}$)TiO$_3$ at 1400 °C, the dielectric constant, dielectric loss, tunability, Curie point, and figure of merit (FOM) were 1400, 0.0027, 18%, −40 °C, and 67, respectively. These compositions show excellent dielectric properties than those of (Ba$_{0.5}$Sr$_{0.5}$)TiO$_3$ ferroelectrics, which are limelight materials for tunable devices such as varactors, phase shifters, and frequency agile filters. © 2009 The Japan Society of Applied Physics

1. Introduction

The barium strontium titanate (BST) ferroelectric system with high dielectric constant is one of the attractive candidate materials for tunable high-frequency devices and dynamic random access memory (DRAM) applications. The BST system has a strong response to the applied dc electric field. This property is very fascinating and has been used to develop devices operating in the microwave region such as phase shifters, frequency agile filters, and tunable capacitors.[1] Ferroelectric materials for these devices should have low dissipation factors (tan δ < 0.01), high tenability, and high figure of merit (FOM) at microwave frequencies.[2] There have been many studies on the development of the dielectric and tunable properties of ferroelectric BST materials because of their large field dependence permittivity and intrinsically fast field response. However, the high dielectric loss of BST materials, particularly in the microwave frequency range, limits their further development.[2,3] In general, Ba$_{0.6}$Sr$_{0.4}$TiO$_3$ was chosen as the basic composition because of its good ferroelectric properties. However, this BST system has a slightly high dielectric loss despite having high tunability. For this reason, BST has a low FOM at microwave frequencies. It is well known that T_c and the dielectric properties of BaTiO$_3$ can be systematically changed by chemical substitution of barium and/or titanium by a wide variety of isovalent and aliovalent dopants.[2,4] The purpose of the present work is to find new ferroelectric materials having excellent ferroelectric properties for tunable devices, such as phase shifters, frequency agile filters, and tunable capacitors. In this paper we report the effect of Sn^{4+} substitution for Ti^{4+}, up to 30 mol %, on ferroelectric properties and dielectric tunability of ceramics in the Ba$_{0.6}$Sr$_{0.4}$TiO$_3$ system.

2. Experimental Procedure

(Ba$_{0.6}$Sr$_{0.4}$)(Ti$_{1-x}$Sn$_x$)O$_3$ (0 ≤ x ≤ 0.3) ceramics were synthesized by the conventional solid-state reaction method and the starting materials were SrCO$_3$, TiO$_2$, SnO$_2$ (Aldrich, 99.9%), and BaCO$_3$ (Aldrich, 99%). These were mixed in a ball mill with ethanol, then dried and calcined in an alumina crucible at 1000 °C for 6 h in air. The calcined powder was remilled with 5 wt % poly(vinyl alcohol) (PVA) as a binder. The powder was pressed uniaxially under a pressure of 1000 kg/cm^2. The resulting pellets with 18 mm diameter and 1–2 mm thickness were sintered at 1350–1400 °C for 2 h in air. The heating and cooling rates were both 5 °C/min. Silver paste electrodes were painted on both sides of sintered ceramic specimens for ferroelectric measurements. Bulk density was measured by the Archimedes method using distilled water as medium. X-ray diffraction (XRD) analysis was carried out on powders for phase identification and lattice parameter measurements.

The capacitance and loss tan δ of the samples were measured using an impedance analyzer (HP4192A) at 1 MHz frequency. The capacitance was also measured under various temperatures. The polarization–electric field (P–E) hysteresis loops were measured using a modified Saw-Tower circuit. Sintered ceramics were examined by powdered XRD (Rigaku Rint/Dmax 2500) analysis with Cu Kα radiation. The microstructure of ferroelectric ceramics was investigated using a scanning electron microscope (SEM; Hitachi S-4200).

3. Results and Discussion

Figure 1 shows XRD spectra for (Ba$_{0.6}$Sr$_{0.4}$)(Ti$_{1-x}$Sn$_x$)O$_3$ (0 ≤ x ≤ 0.3) ceramics sintered at 1400 °C for 2 h. The sintered (Ba$_{0.6}$Sr$_{0.4}$)(Ti$_{1-x}$Sn$_x$)O$_3$ ceramics were a single phase of a cubic (Pm3m) structure. The XRD results indicated that single-phase (Ba$_{0.6}$Sr$_{0.4}$)(Ti$_{1-x}$Sn$_x$)O$_3$ (0 ≤ x ≤ 0.3) solid solutions were synthesized at all compositions. All peaks were slightly shifted to a low angle because larger Sn^{4+} ions (0.69 Å) substituted into B-sites (Ti^{4+}) with a smaller ionic radius (0.61 Å). The lattice parameters were calculated by the least squares method and are shown in Table I. The lattice parameter of (Ba$_{0.6}$Sr$_{0.4}$)(Ti$_{1-x}$Sn$_x$)O$_3$ ceramics increased from 3.955 to 3.997 Å with increasing Sn concentration.

The bulk densities of (Ba$_{0.6}$Sr$_{0.4}$)(Ti$_{1-x}$Sn$_x$)O$_3$ (0 ≤ x ≤ 0.3) ceramics sintered at 1350–1400 °C for 2 h are shown in Fig. 2. The bulk density increased from 5.57 to 5.67 g/cm^3 with increasing Sn concentration from 0 to 0.15 mol and then decreased to 5.43 g/cm^3 with increasing Sn concentration until 0.3 mol. The relative density decreased from 97.3 to 89.1%[5] and well sintered samples were obtained in the range of 0 ≤ x ≤ 0.15. The samples over $x = 0.2$ showed

*E-mail address: jwchoi@kist.re.kr
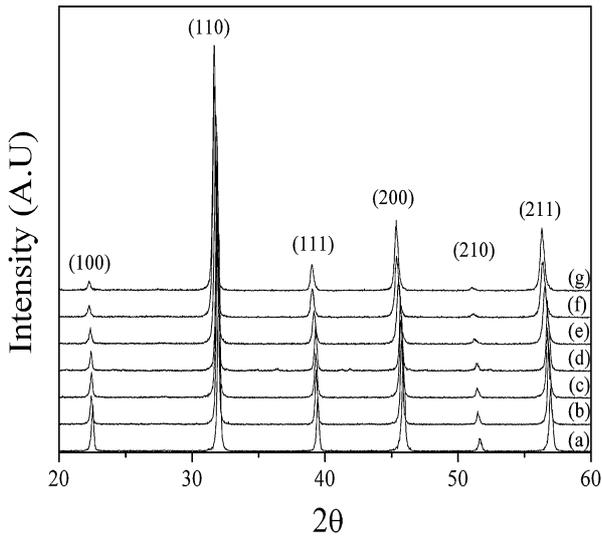
Fig. 1. XRD patterns for specimen of $(Ba_{0.6}Sr_{0.4})(Ti_{1-x}Sn_x)O_3$ sintered at 1400 °C for 2 h: (a) 0, (b) 0.05, (c) 0.1, (d) 0.15, (e) 0.2, (f) 0.25, and (g) 0.3 mol.

Table I. Lattice parameters of $(Ba_{0.6}Sr_{0.4})(Ti_{1-x}Sn_x)O_3$ ceramics sintered at 1400 °C for 2 h.

Sn mol	0	0.05	0.1	0.15	0.2	0.25	0.3
a (Å)	3.9550	3.9638	3.9690	3.9708	3.9820	3.9938	3.9970
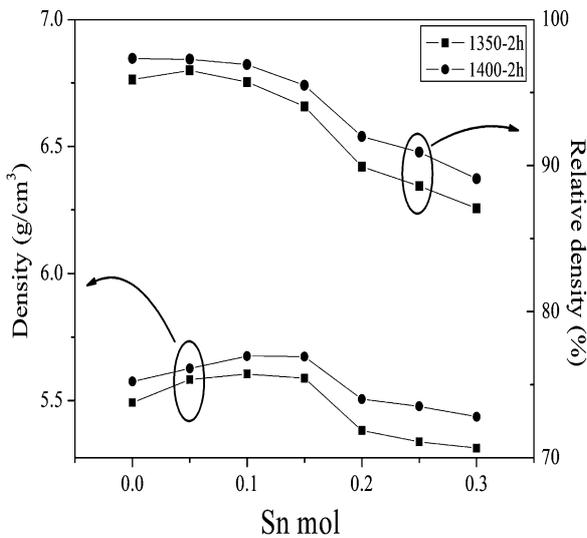
Fig. 2. Densities of $(Ba_{0.6}Sr_{0.4})(Ti_{1-x}Sn_x)O_3$ ceramics sintered at various temperatures for 2 h.

Fig. 3. Curie temperatures of specimen of $(Ba_{0.6}Sr_{0.4})(Ti_{1-x}Sn_x)O_3$ sintered at 1400 °C for 2 h at 1 MHz.
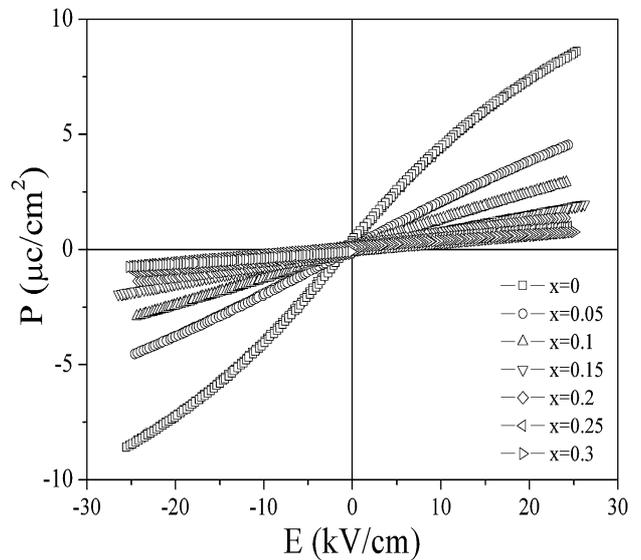
Fig. 4. *P*–*E* field hysteresis loops of $(Ba_{0.6}Sr_{0.4})(Ti_{1-x}Sn_x)O_3$ ceramics sintered at 1400 °C for 2 h.

a lower density, however, the secondary phase was not observed (Fig. 1).

Figure 3 shows the temperature dependence of capacitance of $(Ba_{0.6}Sr_{0.4})(Ti_{1-x}Sn_x)O_3$ ceramics sintered at 1400 °C for 2 h as a function of x measured at 1 MHz. The Curie temperature shifted in the negative direction from 2 to −151 °C with increasing Sn concentration from 0 to 0.3 mol. At higher Sn concentrations (Sn > 0.1), a phase transition showing broad capacitance maxima is called a diffuse phase transition.[6,7] According to Tang *et al.*,[8] in the solid solution of $(Ba_{0.6}Sr_{0.4})(Ti_{1-x}Sn_x)O_3$, Ba and Sr ions occupy the A sites of the ABO$_3$ perovskite structure. Sn and Ti ions occupy the B sites, and the ionic radius of Sn^{4+} (0.69 Å) is

larger than that of Ti^{4+} (0.609 Å); therefore, at higher Sn contents, the $(Ba_{0.6}Sr_{0.4})(Ti_{1-x}Sn_x)O_3$ bulk ceramics show a broad capacitance–temperature curve at the vicinity of the transition temperature T_m, which is caused by an inhomogeneous distribution of Sn ions in the Ti sites and mechanical stress in the grain. According to Yang *et al.*,[9] the diffused phase transition effected by the local polar clusters or regions used to be the existence of weak butterfly hysteresis even at a temperature above T_m. However, in this system, the weak butterfly hysteresis was not observed as Sn concentration increased. This absence of weak butterfly hysteresis is suitable for tunable devices.

The *P*–*E* hysteresis loops of $(Ba_{0.6}Sr_{0.4})(Ti_{1-x}Sn_x)O_3$ ceramics measured at room temperature are shown in Fig. 4. The slim hysteresis loop with almost zero remnant polarization indicated that $(Ba_{0.6}Sr_{0.4})(Ti_{1-x}Sn_x)O_3$ ceramics existed in the paraelectric phase at room temperature. It is known that the polarization described as
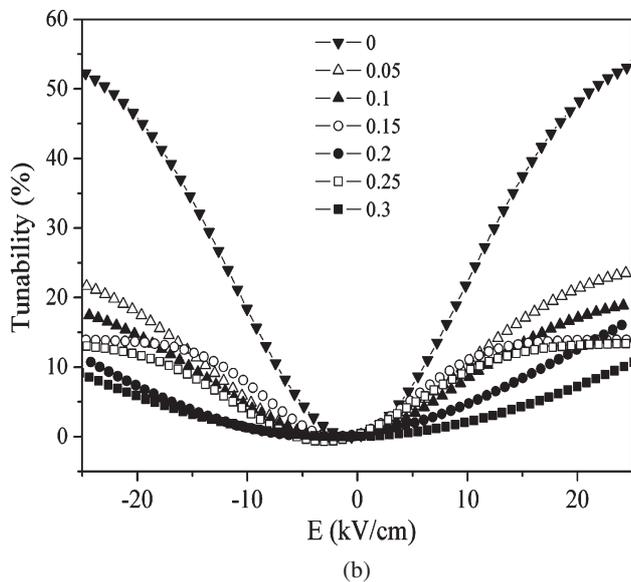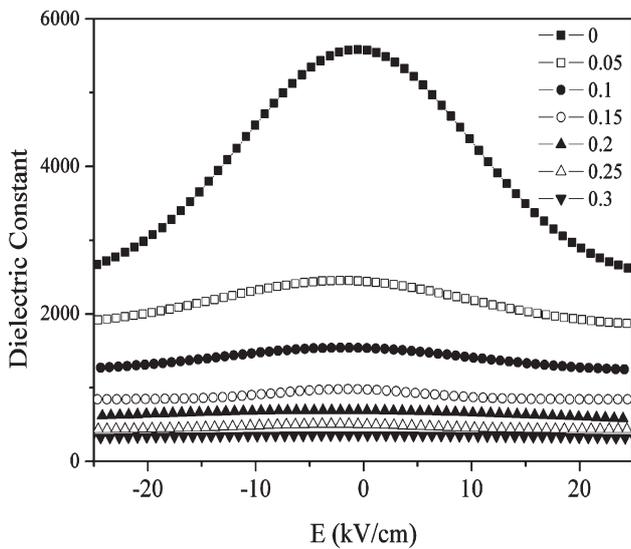
Fig. 5. (a) Dielectric constants and (b) tunabilities of $(Ba_{0.6}Sr_{0.4})$-$(Ti_{1-x}Sn_x)O_3$ ceramics sintered at 1400 °C for 2 h.

$$P = \varepsilon_0(K-1)E. \qquad (1)$$

Here, P is the polarization, E is the applied electric field, ε_0 is the vacuum permittivity, and K is the dielectric constant, respectively. From eq. (1), the dielectric constant was calculated from the slope of the P–E hysteresis loop. The dielectric constant vs the electric field of $(Ba_{0.6}Sr_{0.4})(Ti_{1-x}Sn_x)O_3$ ceramics and tunability as a function of x measured at $E = 25\,kV/cm$ is shown in Fig. 5. Tunability can be calculated using

$$\text{Tunability (\%)} = \frac{K_0 - K_v}{K_0} \times 100. \qquad (2)$$

Here, K_0 and K_v represent the dielectric constant at zero and applied electric field, respectively. At room temperature, the tunability of $(Ba_{0.6}Sr_{0.4})(Ti_{1-x}Sn_x)O_3$ ceramics decreases with increasing Sn content. The tunabilities measured at room temperature under a biasing field of $E = 25\,kV/cm$ for $(Ba_{0.6}Sr_{0.4})(Ti_{1-x}Sn_x)O_3$ ceramics are 52% ($x = 0$), 23% ($x = 0.05$), 18% ($x = 0.1$), and 9% ($x = 0.3$), respectively.
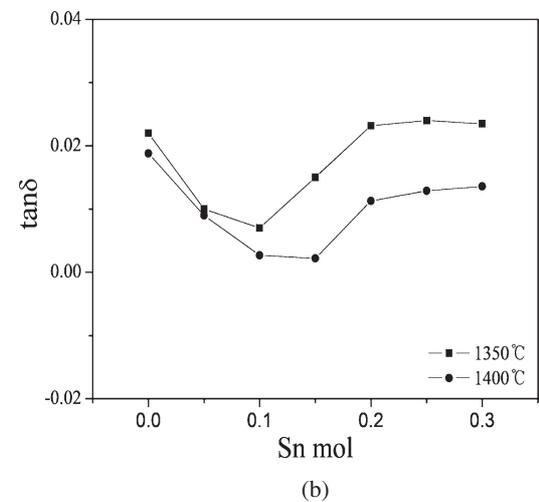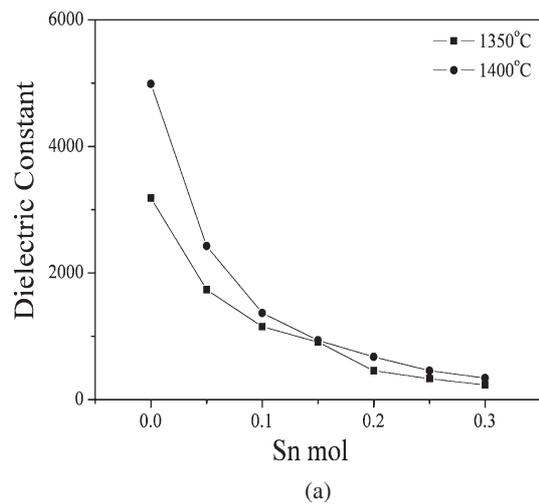
Fig. 6. (a) Dielectric constants and (b) dielectric losses of $(Ba_{0.6}$-$Sr_{0.4})(Ti_{1-x}Sn_x)O_3$ ceramics sintered at various temperatures for 2 h.

The high tunability of the $(Ba_{0.6}Sr_{0.4})TiO_3$ ceramics near the transition temperature is expected because the permittivity become very high and the polarization that can be induced by even a small field can be quite large at a temperature near to the transition temperature.[8–10]

Figure 6 shows the dielectric constants and losses (tan δ) of $(Ba_{0.6}Sr_{0.4})(Ti_{1-x}Sn_x)O_3$ ceramics sintered at various temperatures for 2 h as a function of x at 1 MHz. The dielectric constant of $(Ba_{0.6}Sr_{0.4})(Ti_{1-x}Sn_x)O_3$ ceramics sintered at 1400 °C for 2 h decreased from 4990 to 340. It is expected that the decrease in dielectric constant by substitution of Sn occurs because a slightly large Sn^{4+} ion (0.69 Å) is incorporated to a B-site (Ti^{4+}) with a slightly smaller ionic radius (0.609 Å); hence, the ion is not easily displaced under an electric field. This result is reasonable when we consider that an increase in Sn concentration slightly decreased the dielectric constant, as reported by Kucheiko *et al.*[5,11] The dielectric loss decreased from 0.019 to 0.0022 with increasing Sn concentration from 0 to 0.15 mol and then increased to 0.0136 with Sn concentration until 0.3 mol. The element tin (Sn) is capable of forming +2 and +4 ions, which occurs both in the solid state and in solution.[11] Hu *et al.*[12] suggested that the oxidation state +4 involves both the s- and p-electrons. The oxidation state +2, involving only the p-electrons, and the two s-electrons are retained as an inert

pair. As a Sn ion changes from +4 to +3 (or +2), the oxygen vacancy is pinned, which decreases dielectric loss.

On the other hand, the relationship between $\tan\delta$ and substitution of Sn ions revealed the same trend as the relationship between bulk density and Sn concentrations. It was noteworthy that Sn concentration decreased the dielectric loss of $(Ba_{0.6}Sr_{0.4})(Ti_{1-x}Sn_x)O_3$ ceramics, which have good sinterability (over 95%).[13] The dielectric losses of $(Ba_{0.6}Sr_{0.4})(Ti_{0.9}Sn_{0.1})O_3$ ceramics decreased from 0.007 to 0.002 with increasing sintering temperature. The dielectric loss is affected by the grain boundary. The grain size slightly increased from 2 to 3 um at sintering temperatures of 1350 and 1400 °C, respectively. Over the 0.2 mol of Sn, however, the dielectric loss of the ceramics increased as the sinterability decreased. From this result, the sinterability of ceramics is mainly the predominant factor for improving the dielectric loss of ferroelectric materials.

FOM is calculated using

$$FOM = Tunability \ (\%)/\tan\delta. \qquad (3)$$

The values of FOM are shown in Fig. 7, which is calculated at room temperature and under a bias field of 25 kV/cm. The maximum value of FOM (67) is found at $x = 0.1$. The result also implies that the optimum conditions of the ceramics for possible tuning applications at room temperature can be found at $x = 0.1$.

4. Conclusions

The dielectric properties of $(Ba_{0.6}Sr_{0.4})(Ti_{1-x}Sn_x)O_3$ ($0 \leq x \leq 0.3$) ceramics were investigated. Single-phase specimens having a cubic perovskite structure were obtained. As Sn concentration increased, the dielectric loss decreased untill a composition of $x = 0.15$ and then slightly increased, and the Curie temperature was suppressed. According to substitution of Sn ions, the diffused phase transition appeared. When Sn was substituted at 0.05 and 0.1 mol in the BST system at 1400 °C, the dielectric constant, dielectric loss, tunability, Curie point, and FOM were 2500 and 1400, 0.009 and 0.0027, 23 and 18%, −18 and −40 °C, and 25 and 67, respectively.
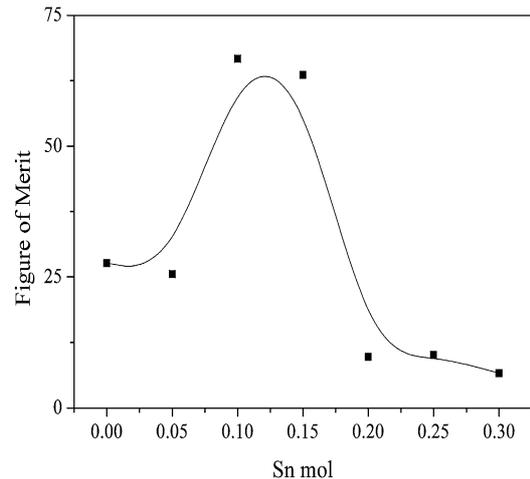
Fig. 7. FOM values of $(Ba_{0.6}Sr_{0.4})(Ti_{1-x}Sn_x)O_3$ ceramics sintered at 1400 °C for 2 h.

1) A. K. Tagantsev, V. O. Sherman, K. F. Astafiev, J. Venkatesh, and N. Setter: J. Electroceram. **11** (2003) 5.
2) L. C. Sengupta and S. Sengupta: Mater. Res. Innovations **2** (1999) 278.
3) X. Liang, Z. Meng, and W. Wu: J. Am. Ceram. Soc. **87** (2004) 2218.
4) A. Feteira, D. C. Sinclair, I. M. Reaney, Y. Somiya, and M. T. Lanagan: J. Am. Ceram. Soc. **87** (2004) 1082.
5) S. Kucheiko, J.-W. Choi, H.-J. Kim, S.-J. Yoon, and H.-J. Jung: J. Am. Ceram. Soc. **80** (1997) 2937.
6) G. A. Smolenskii and V. A. Isupov: Sov. Phys. Dokl. **9** (1954) 653.
7) G. A. Smolenskii and V. A. Isupov: Sov. Phys. Tech. Phys. **24** (1954) 1375.
8) X. G. Tang, K.-H. Chew, and H. L. W. Chan: Acta Mater. **52** (2004) 5177.
9) J. Yang, J. Chu, and M. Shen: Appl. Phys. Lett. **90** (2007) 242908.
10) M. E. Lines and A. M. Glass: *Principles and Applications of Ferroelectrics and Related Materials* (Oxford University Press, Oxford, U.K., 2001) p. 77.
11) C. Chambers and A. K. Holliday: in *Modern Inorganic Chemistry* (Butterworth & Co., London, 1975) p. 160.
12) W. Hu, C. Yang, X. Liu, W. He, and X. Tang: J. Mater. Sci.: Mater. Electron. **19** (2008) 61.
13) J.-W. Choi, C.-Y. Kang, S.-J. Yoon, H.-J. Kim, H.-J. Jung, and K. H. Yoon: J. Mater. Res. **14** (1999) 3567.